Veterinary Immunology and Immunopathology 208 (2019) 25–33

Contents lists available at ScienceDirect

Veterinary Immunology and Immunopathology

journal homepage: www.elsevier.com/locate/vetimm

Research paper

Insights into the intestine immune of *Marsupenaeus japonicus* under the white spot syndrome virus challenge using RNA sequencing

Kaimin Hui[a], Qian Ren[a,b,*], Jun Cao[a,*]

[a] College of Marine Science and Engineering, Nanjing Normal University, Institute of Life Sciences, Jiangsu University, Zhenjiang, Jiangsu, People's Republic of China
[b] Co-Innovation Center for Marine Bio-Industry Technology of Jiangsu Province, Lianyungang, Jiangsu, People's Republic of China

ARTICLE INFO

Keywords:
Marsupenaeus japonicus
Intestine immune
WSSV
Transcriptome

ABSTRACT

Intestine is not only the nutrients digestion and absorption centers, but also an important place of microbial infection. Therefore, intestine immunity plays a key defense means for the host against the invasion of pathogenic microorganisms. In this study, we use kuruma shrimp (*Marsupenaeus japonicus*) as a model to study the intestine immune characteristics of shrimp against WSSV through next-generation sequencing technique. A total of 63,458 and 44,350 unigenes were generated from the control sample and the WSSV infection sample, respectively. Based on homology searches, KEGG, GO, and COG analysis, 39,520 unigenes were annotated. Among them, 12,920 differentially expressed genes were identified. Some of them, including mucin, peritrophin, chitinase, et al., are involved in immune response. These results contribute to a better understanding of the intestine immune response of the shrimp to WSSV.

1. Introduction

The intestine is not only an important place for digestion and absorption of nutrients, but also the main immune organ of organisms (Wittig and Zeitz, 2003). The intestinal immune system consists of three components: mechanical barrier composed of intestinal mucosal cells; immune barrier composed of intestinal immune cells and their secretions; and biological barrier composed of normal intestinal flora (Yan et al., 2013). The three barriers not only maintain the important physiological function of intestinal tract, such as protecting the organism's digestion and absorption of nutrients, but also play the intestinal immune defense function, such as, maintaining the intestinal microbial ecological balance, and resisting foreign invasion of pathogenic bacteria (Faderl et al., 2015). The intestinal mucosal area is large, and its structure and function constitute a powerful mucosal immune system (Ménard et al., 2010). The intestinal immune system of the crustacean is a complex structure composed of intestinal epithelial cells, which are closely connected with each other, mucus secreted by ring-shaped cells, and bioactive proteins secreted by intestinal epithelial cells. In addition, there are a large number of symbiotic bacterial existing in the intestine. They can not only effectively prevent pathogenic bacteria from adhesion and invasion into intestinal epithelial cells, but also produce immune related cytokines killing pathogens (Ménard et al., 2010; Gill et al., 2010). Therefore, the intestinal immune system is an important defense line for crustaceans to resist foreign pathogenic microorganisms invading the host.

Marsupenaeus japonicus, also know as kuruma shrimp, is one of the most important aquaculture shrimp species worldwide. However, frequent disease outbreaks caused by bacteria and viruses have led to high mortality of shrimp and a great economic loss, which have seriously restricted the development of shrimp farming industry (Seibert and Pinto, 2012). White spot syndrome virus (WSSV) was first appeared in 1992. As a rapidly replicating and extremely virulent pathogen, WSSV is the most serious disease-causing agent in shrimp aquaculture worldwide (Lo et al., 1996). All decapod crustaceans, including crabs, crayfishes, and shrimp, are considered susceptible to this virus. Moreover, the virus can cause over 90% mortality in farmed shrimp (Wang et al., 1998).

Transcriptome analysis using the next-generation sequencing is an efficient way to rapidly generate large amounts of data with low cost (Mutz et al., 2013). This approach has been used to discover the molecular basis of some immune processes (Rao et al., 2015; Chen et al., 2016; Cao et al., 2017). However, no information is available on the gene expression profiles of *M. japonicus* intestine organs with a WSSV infection. In the present study, next-generation sequencing and bioinformatics techniques were applied to compare the transcriptome differences between the WSSV-infected and uninfected shrimp intestine organs. It will demonstrate some molecular mechanisms of intestine

* Corresponding authors at: College of Marine Science and Engineering, Nanjing Normal University, Institute of Life Sciences, Jiangsu University, Zhenjiang, Jiangsu, People's Republic of China.
E-mail addresses: renqian0402@126.com (Q. Ren), cjinfor@163.com (J. Cao).

https://doi.org/10.1016/j.vetimm.2018.12.001
Received 23 March 2018; Received in revised form 23 November 2018; Accepted 3 December 2018

immune against WSSV infection and construct possible strategies to prevent the spread of the virus in aquaculture.

2. Materials and methods

2.1. M. japonicus preparation and WSSV infection

Shrimp (*M. japonicus*) was purchased from a local aquaculture farm in Hangzhou, Zhejiang Province, China. The shrimp was divided into two groups (WSSV challenged group and PBS challenged group). Each group (15 individuals) was cultured in the same tank filled with seawater at room temperature; the shrimp was acclimatized for 3 days prior to the experiments. In order to ensure that the shrimp used in the experiments was free of WSSV, genome DNA extracted from gills of three randomly selected shrimp was used for PCR detection of WSSV copies using WSSV-specific primers. In WSSV challenged group, each virus-free shrimp was challenged with 10^4 copies of virus by injecting with 100 μl of WSSV solution (10^5 copies/ml) into the lateral area of the fourth abdominal segment. WSSV was obtained from a lab in Zhejiang University and the virus was extracted from the tissues of an infected crayfish, *Procambarus clarkii*. Detailed methods of virus extraction and quantification could be seen a previously published paper (Ye et al., 2012). In the PBS challenged group, each shrimp was injected with 100 μl of PBS instead of virus. The response of shrimp to pathogens varies greatly among individuals. In order to reduce the experimental error, we put several shrimps together for transcriptome sequencing. After 48 h of WSSV or PBS challenge, the intestine from 3 shrimp was dissected and mixed as one sample for RNA extraction. And equimolar amount of RNA was pooled for transcriptome sequencing.

2.2. RNA extraction, cDNA library construction, and sequencing

We used high-purity total RNA Rapid Extraction Kit (BioTeke, Beijing, China) to extract total RNA from WSSV-infected and control samples according to the manufacturer's instructions. 1% formaldehyde agarose gel electrophoresis (15 min) was performed to check total RNA quality, and RNA concentration was determined through NanoDrop (Thermo Scientific). PrimeScript 1 st Strand cDNA Synthesis Kit (Dalian, China) was then used for first-strand cDNA synthesis with random oligonucleotides. Next, DNA polymerase I was used to perform second-strand cDNA synthesis, which was further phosphorylated and added 'A' base. Finally, the Illumina Hiseq2000 platform was used to sequence this library at BGI Co., Ltd. (Shenzhen, China).

2.3. De novo assembly and data analysis

SeqPrep (http://github.com/jstjohn/SeqPrep) and Sickle (https://github.com/najoshi/sickle) were used to process the raw reads with default parameters and sequences smaller than 60 bases were eliminated. Next, RNA assembly of clean data from the mock and WSSV-infected samples was performed with Trinity Program (Grabherr et al., 2011). Seven functional databases (NCBI protein NR, NT, Swissprot, KEGG, COG, Interpro, and GO) were used for searching the assembled transcripts. The function annotations were retrieved based on the highest sequence similarity and a typical cut-off *E*-value < 1.0 E^{-5} (Mortazavi et al., 2008). In addition, we also used the Blast2GO Program (Conesa et al., 2005) and KEGG (http://www.genome.jp/kegg/) to perform GO annotations of the uniquely assembled transcripts and metabolic pathway analysis, respectively.

2.4. Differential expression analysis and functional annotation

FPKM (fragments per kilobase of transcripts per million fragments mapped) was used as the measurement unit to estimate the expression level of each transcript in this study. Furthermore, false discovery rate (FDR) was also used to correct for *E*-value. Genes with FDR ≤ 0.001 and an FPKM ratio ≥ 2 or ≤ 0.5 were considered as DEGs (differential expression genes) between the infected and uninfected samples. In addition, KEGG and GO were also used for DEG pathway and GO enrichment analysis, respectively.

Table 1
Primers used in this study.

Primer names	Sequences (5`–3`)
MjALF6-RT-F	GCCAAGCTCAGGGACTAAA
MjALF6-RT-R	ACAGGTGATCTAGCAGGTCTA
MjALF1-RT-F	GGCGAAAGGGAAATGTTTGG
MjALF1-RT-R	GCAGGTCATCCTTCCCTTAAA
MjKPI-RT-F	TCTGTTTAGCCCTGTGTGTG
MjKPI-RT-R	CAAGAAACGTCAGCCACTTTG
MjTrx-RT-F	GTGAAAGGAGGGAAGGTTGTAG
MjTrx-RT-R	CAATCAGCCTCCCGACAAA
MjUbc-RT-F	CTCCCAGAGTATGGCACTAAAG
MjUbc-RT-R	TGAAAGAGGTCGTCTCCTACT
MjGAPDH-RT-F	TGAGCAAGACCTTCGTCAAG
MjGAPDH-RT-R	GGCATCAATCTTCTGCATGTG

Table 2
Statistics of the transcriptome sequencing results.

Samples		Mock	WSSV-infected
Raw reads		56.05 Mb	55.97 Mb
Clean reads		56.05 Mb	55.97 Mb
Clean bases		8.41 Gb	8.40 Gb
Q20 (%)		97.09	97.62
GC (%)		43.3	42.82
Unigene	Total Num	63,458	44,350
	Total bases	54,424,461	34,170,976
	Mean length	857	770
All	Total Num	66,367	
	Total bases	59,205,696	
	Mean length	892	

2.5. Validation of genes using qRT-PCR

A total of five differentially expressed unigenes from the intestine transcriptome data of shrimp (*M. japonicus*) were selected for quantitative RT-PCR (qRT-PCR) analysis to validate the Illumina sequencing results. These five genes are as below: *anti-lipopolysaccharide factor* (*ALF*) *6* (*MjALF6*), *MjALF1*, *kazal-type proteinase inhibitor* (*MjKPI*), *thioredoxin* (*MjTrx*) and *ubiquitin-conjugating enzyme* (*MjUbc*). When performing qRT-PCR analysis, *glyceraldehyde-3-phosphate dehydrogenase* (*MjGAPDH*) was also amplified as an internal control gene. All primers used in the qRT-PCR analysis are listed in Table 1. In order to conduct the qRT-PCR experiments, total RNA was first isolated from the intestine of experimental (48 h WSSV-challenged intestine) and mock (48 h PBS-challenged intestine) shrimp using a high-purity total RNA Rapid Extraction Kit (BioTeke, Beijing, China). Three biologically repeated samples were prepared for the experiment and the control group. High quality of RNA was then transcribed into the first-strand cDNA using EasyScript One-Step gDNA Removal and cDNA Synthesis SuperMix (TransGen Biotech, China) according to the manufacturer's instructions. The prepared cDNA was then used for qRT-PCR analysis using TransStart Green qPCR SuperMix (TransGen Biotech, China). $2^{-\Delta\Delta Ct}$ method was used to calculate the relative changes of gene expression (Livak and Schmittgen, 2001). The values of log 2-fold changes were used for making histogram.

3. Results and discussion

3.1. Transcriptome sequencing and de novo assembly

We used the Illumina Hiseq2000 sequencing platform to perform

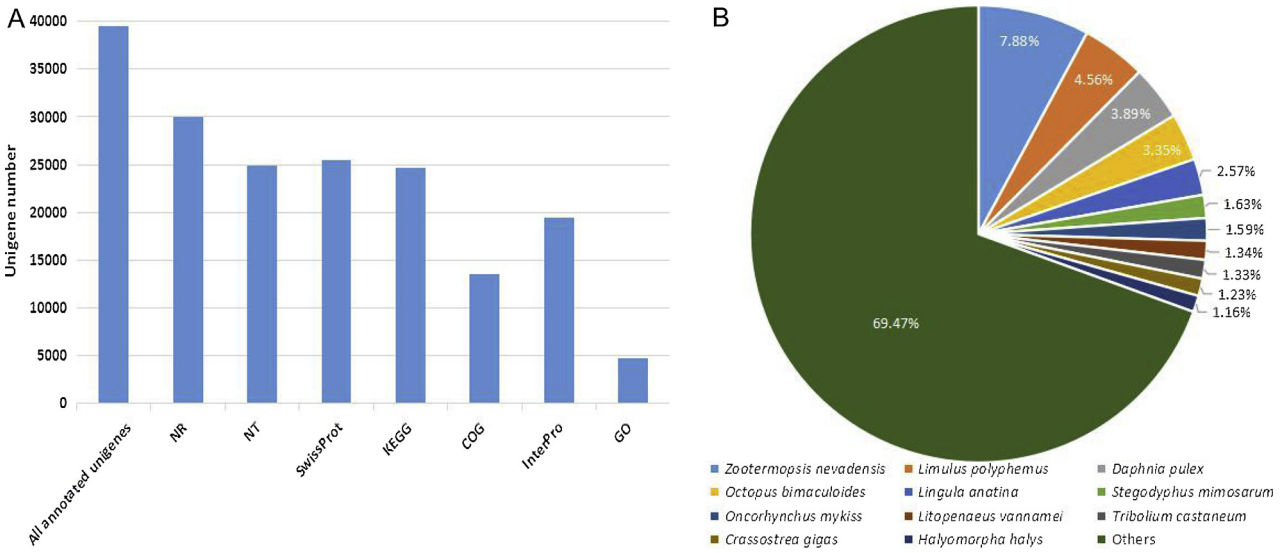

Fig. 1. Homology search of *M. japonicus*. (A) Annotation statistics of *M. japonicus* transcriptome in NR, NT, SwissProt, KEGG, COG, InterPro and GO databases; (B) Species distribution of the unigene dataset by aligning sequences against the NR protein database. The eleven top-hit species based on NR annotation are shown here.

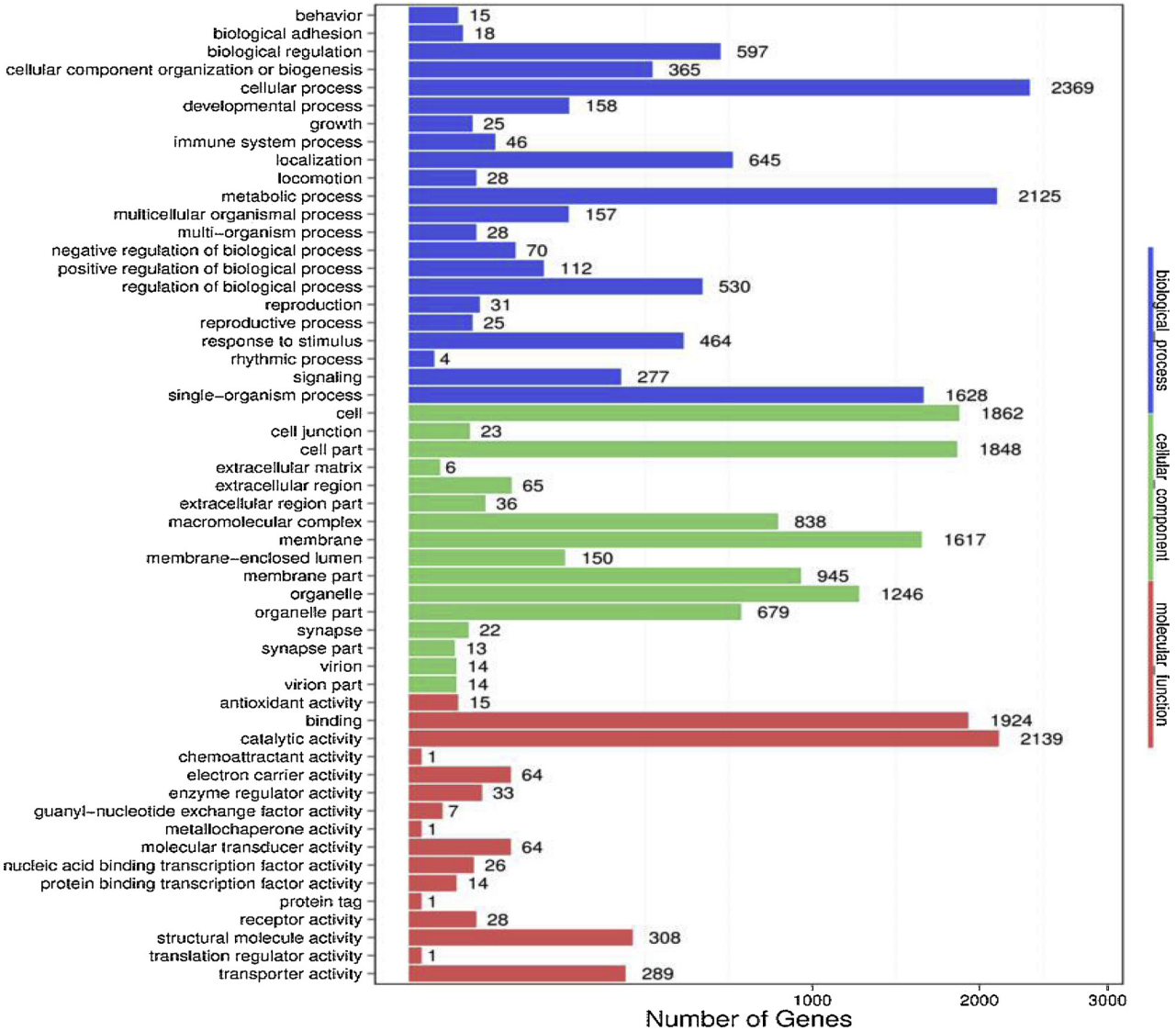

Fig. 2. Gene ontology (GO) classification of all unigenes. The X-axis represents number of unigenes and Y-axis indicates the GO categories. Three main GO categories (biological processes, cellular component, and molecular function) are shown by different color bars.

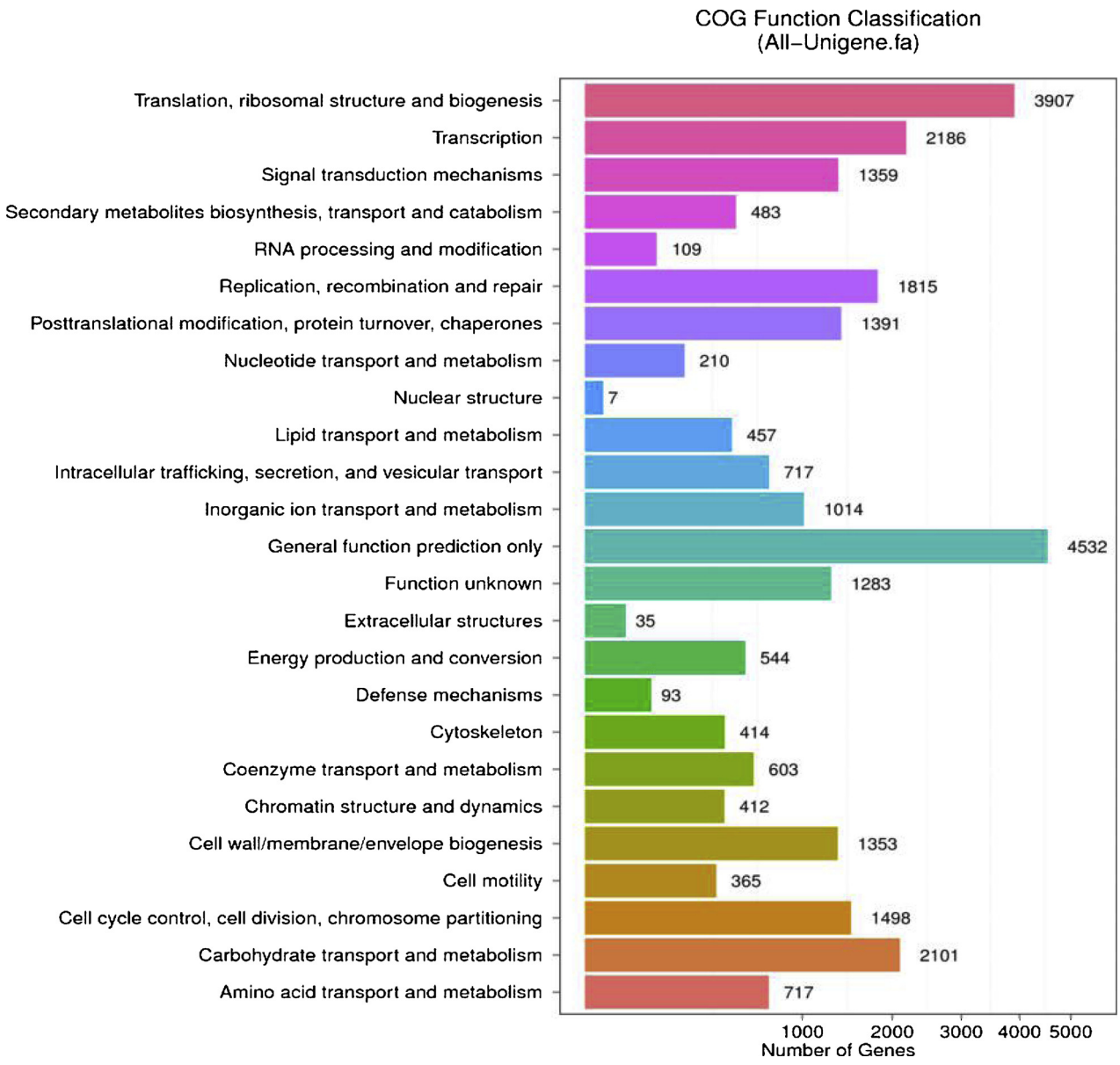

Fig. 3. COG function classification of *M. japonicus* transcriptome. The X-axis represents numbers of unigenes and Y-axis stands for the 25 different functional categories.

high-throughput sequencing for WSSV-infected and mock intestine samples of *M. japonicus*. As a result, 56.05 Mb (8.41 Gb nucleotides) and 55.97 Mb (8.40 Gb nucleotides) clear reads were produced in the mock and WSSV-infected samples after removal of low-quality sequences, respectively (Table 2). The GC content of nucleotide was 43.3% and 42.82% in the mock and WSSV-infected groups, respectively. With the Trinity program (Grabherr et al., 2011), the transcriptome assembly yielded 63,458 and 44,350 unigenes with a mean length of 857 and 770 nucleotides for control and WSSV-infected samples, respectively, whereas assembly of a combined two-sample transcriptome generated 66,367 unigenes with an average of 892 nucleotide lengths (Table 2). Among them, the 49,869 unigenes (75.14%) were less than 1000 bps, and 37,407 ones (56.36%) were less than 500 bps (Fig. S1). Previous transcriptome data have assembled about 67,284 genes on the hemocytes of *M. japonicus* (Koiwai et al., 2018b), which is similar to our experimental result. While the same group only got 44,088 transcripts on the phagocytic hemocytes by RNA-seq analysis (Koiwai et al., 2018a). The difference on gene number may be due to the different shrimp tissues or under different treatments.

3.2. Functional annotation and classification of M. japonicus transcriptome sequences

Protein annotation can provide some functional and expression information. In this study, all 66,367 unigene sequences were first aligned to the NCBI nonredundant (NR), COG, SwissProt, KEGG, and InterPro databases by BLASTX, and nucleotide database (NT) (*E*-value < 1.0 E^{-5}) by BLASTN. Annotation information was retrieved from protein with the highest sequence similarity. In total, 39,520 (59.55%) unigenes were annotated. Among them, 29,961 (75.81%) assembled unigenes aligned to the NR protein database, whereas only 4756 (12.03%) unigenes aligned to the GO database (Fig. 1A). Previous study has indicated that about 17,000 unigenes were annotated from a transcriptome analysis of the shrimp hepatopancreas challenged by WSSV (Zhong et al., 2017). It suggested that compared with the hepatopancreas immune, there may be more genes involved in the intestinal immune of the shrimp. Next, to further study the sequence conservation, we also compared the species distribution of the unigenes. The result indicated that over 30.53% of the total unigenes matched with

Table 3
KEGG classification of *M. japonicus* unigenes.

KEGG categories	No. of unigenes (%)	KEGG categories	No. of unigenes (%)
Human Dseases	**12019 (25.88%)**	Lipid metabolism	747 (1.61%)
Infectious diseases	4610 (9.92%)	Nucleotide metabolism	605 (1.30%)
Cancers	3925 (8.45%)	Glycan biosynthesis and metabolism	444 (0.96%)
Neurodegenerative diseases	1209 (2.60%)	Metabolism of cofactors and vitamins	368 (0.79%)
Endocrine and metabolic diseases	677 (1.46%)	Energy metabolism	354 (0.76%)
Cardiovascular diseases	525 (1.13%)	Metabolism of other amino acids	245 (0.53%)
Substance dependence	518 (1.12%)	Xenobiotics biodegradation and metabolism	192 (0.41%)
Antineoplastic resistance	320 (0.69%)	Metabolism of terpenoids and polyketides	80 (0.17%)
Immune diseases	235 (0.51%)	Biosynthesis of other secondary metabolites	34 (0.07%)
Organismal Systems	**9850 (21.21%)**	**Environmental Information Processing**	**6461 (13.91%)**
Endocrine system	1941 (4.18%)	Signal transduction	4955 (10.67%)
Immune system	1565 (3.37%)	Signaling molecules and interaction	1364 (2.94%)
Nerous system	1518 (3.27%)	Membrane transport	142 (0.31%)
Digestive system	1215 (2.62%)	**Genetic Information Processing**	**5078 (10.93%)**
Development	1128 (2.43%)	Translation	2160 (4.65%)
Sensory system	775 (1.67%)	Transcription	1505 (3.24%)
Circulatory system	626 (1.35%)	Folding, sorting and degradation	1035 (2.23%)
Aging	431 (0.93%)	Replication and repair	378 (0.81%)
Excretory system	330 (0.71%)	**Cellular Processes**	**5066 (10.91%)**
Environmental adaptation	321 (0.69%)	Transport and catabolism	1762 (3.79%)
Metabolism	**7975 (17.17%)**	Cell communication	1599 (3.44%)
Global and overview map	3028 (6.52%)	Cell growth and death	906 (1.95%)
Carbohydrate metabolism	1003 (2.16%)	Cell motility	799 (1.72%)
Amino acid metabolism	875 (1.88%)	**Total**	**46449 (100%)**

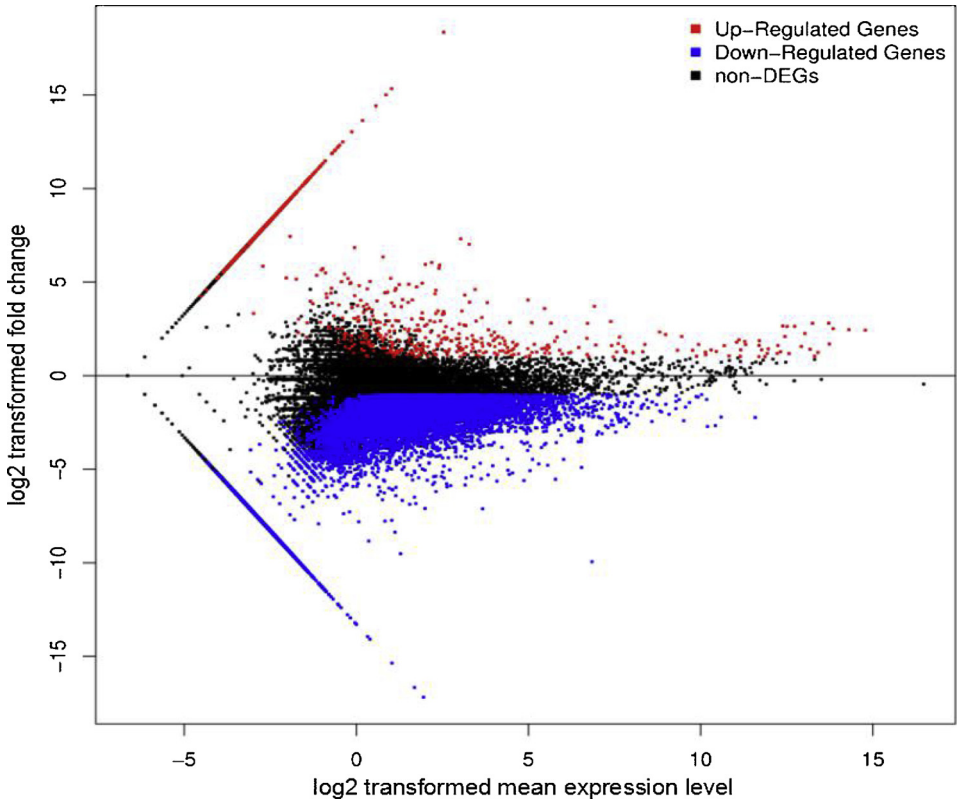

Fig. 4. Visualization of differentially expressed genes (DEGs) between infection and mock groups. Red: up-regulated; Blue: down-regulated; Black: no significant differential expression. (For interpretation of the references to colour in this figure legend, the reader is referred to the web version of this article.)

sequence from the following eleven species: *Zootermopsis nevadensis* (7.88%), *Limulus polyphemus* (4.65%), *Daphnia pulex* (3.89%), *Octopus bimaculoides* (3.35%), *Lingula anatina* (2.57%), *Stegodyphus mimosarum* (1.63%), *Oncorhynchus mykiss* (1.59%), *Litopenaeus vannamei* (1.34%), *Tribolium castaneum* (1.33%), *Crassostrea gigas* (1.23%), and *Halyomorpha halys* (1.16%) (Fig. 1B).

GO classification can describe the function of gene products (Schlicker et al., 2006). To determine the functional genes found in this RNA-seq, we performed GO enrichment analysis. The result revealed that 4756 matched unigenes (7.17% of total unigenes or 12.03% of annotated unigenes) were divided into three GO categories, including 54 functional groups (Fig. 2). Among all 24,010 GO assignments, 40.47% comprised biological processes, 39.06% comprised cellular component, and 20.47% comprised molecular function (Fig. 2). In the category of biological processes, most unigenes were involved in the "cellular process" (24.38%), "metabolic process" (21.87%), and "single-

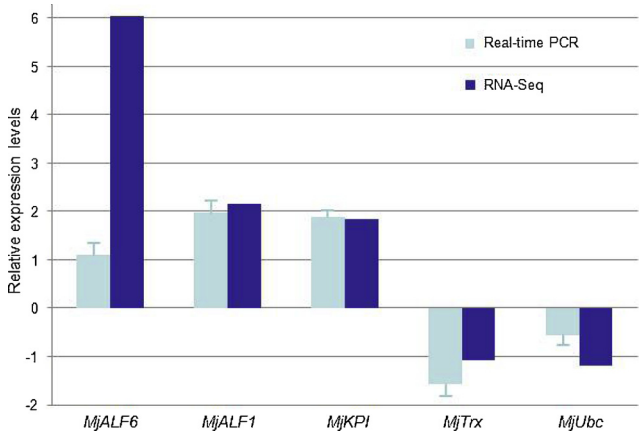

Fig. 5. Comparison of the expression profiles of five selected genes (*MjALF6*, *MjALF1*, *MjKPI*, *MjTrx*, and *MjUbc*) as determined by RNA-seq and real-time PCR.

organism process" (16.75%). With respect to cellular component category, "cell" (19.85%), "cell part" (19.71%), and "membrane" (17.24%) were the dominant groups. In molecular function category, the most represented were "catalytic activity" (43.52%), "binding" (39.15%), and "structure molecule activity" (6.27%) (Fig. 2). The GO classification was similar to the transcriptome studies (Cao et al., 2017; Zhong et al., 2017). These provided abundant data for better understanding the response of crustaceans infected with WSSV, and facilitated the identification of immune related genes.

We also used COG database to indicate 53,134 matched unigenes (80.06% of total unigenes) and resulted in 27,605 functional annotations clustered into 25 categories (Fig. 3). "General functional prediction only" (4,532, 16.42%), "translation, ribosomal structure, and biogenesis" (3,907, 14.15%), and "transcription" (2,186, 7.92%) are the three largest groups. While only 7 unigenes were classed into "nuclear structure". In addition, to further understand the biological function of the unigenes, KEGG database (http://www.genome.jp/kegg/) was also used to identify potential biological pathways in the transcriptome of *M. japonicus* intestine tissue. A total of 16,511 unigenes were assigned into 245 KEGG pathways (Table 3). Moreover, a greater number of genes were associated with human disease (25.88%), organismal system (21.21%), and metabolism processing (17.17%). The results of KEGG enrichment analysis indicated that multiple signaling pathways might involve in the intestine immune processes of the shrimp under WSSV challenge.

3.3. Identification and functional characterization of differentially expressed genes (DEGs)

To identify the DEGs involved in the intestine immune of *M. japonicus* under WSSV challenge, we compared the mock and WSSV-infected samples with a threshold absolute value of $\log_2$ fold-change ≥ 1 and FDR ≤ 0.001 with the FPKM algorithm. As a result, a total of 12,920 DEGs were identified. Among them, only 675 unigenes (5.22%) were up-regulated, and others were down-regulated (Fig. 4). It suggested that the WSSV infection is associated with the reduction of transcripts in the intestine tissue of *M. japonicus*. Next, to further obtain functional information of these DEGs, we also investigated their GO classification. The results indicated that the over-represented GO terms for DEGs were "cellular process", "metabolic process", and "single-organism process" in the biological process category. GO terms "cell," "cell part," and "membrane" were highly represented for DEGs in the cellular component category (Fig. S3). These catalytic and binding-related processes may play important roles in the WSSV response in the intestine organ of *M. japonicus*. In addition, KEGG analysis also identified 5816 DEGs annotated into 222 pathways. Compared with the mock sample, numbers DEGs abnormally expressed in the WSSV-infected sample were involved in various immune processes. These data indicated comprehensive molecular immune mechanisms underlying the response to WSSV infection, similar to previous studies (Pan et al., 2005; Hu and Yao, 2016; Cao et al., 2017; Zhong et al., 2017).

3.4. Validation of RNA-seq results by qRT-PCR

To further validate the results from the RNA sequencing data, five differentially expressed unigenes (3 up-regulated genes and 2 down-regulated genes in 48 h WSSV-challenged intestine transcriptome in compare to the mock one) were selected randomly for qRT-PCR analysis. Specific primers were designed through online software (https://www.idtdna.com/Primerquest/Home/Index). The qRT-PCR analyses were performed in the three biological replicates of each sample. From the qRT-PCR results, it could be seen that all selected 5 genes showed similar expression patterns in the qRT-PCR analysis as observed from RNA-seq data (Fig. 5).

3.5. Up-regulated genes of interest related to immune response against WSSV

The transcriptome of *M. japonicus* intestine tissue against WSSV was examined to identify some candidate genes that might be functionally associated with the immune response. According to our sequence analysis and published literatures, some genes involved in immune response, including mucin, peritrophin, cytochrome c oxidase, chitinase, anti-lipopolysaccharide factor, syndecan, Rho GTPase, and other potential candidates, were identified (Table 4).

The intestine surface is covered with secreted mucus, which can function as a barrier to protect the epithelium from viruses, pathogenic bacteria, and other toxic agents (Hartmann et al., 2013). The mucus is composed of many molecules, including glycoproteins, nucleic acids, lipids, and some salt. The major components of the mucus barrier are gal-forming mucins secreted by goblet cells (Hasnain et al., 2013; Johansson and Hansson, 2016). The mucin sequences contain mucin domains which are extensively decorated by *O*-linked glycans. Therefore, mucins are defined as glycoproteins (Lang et al., 2007). Previous studies have suggested that mucins and their glycans can bind some immune proteins and have immunological effects (McGuckin et al., 2011). Mice with Muc1 deficiency is more susceptible to the infection of pathogens *Helicobacter pylori* and *Campylobacter jejuni* (McGuckin et al., 2007; McAuley et al., 2007). Similarly, Muc2-knockout mice displayed aberrant intestinal morphology and frequently developed colon tumor, suggesting that Muc2 is involved in the suppression of colorectal cancer (Velcich et al., 2002). In addition, mucin-like PM (peritrophic membrane) was also shown to be induced in the digestive organ of the black tiger shrimp, *Penaeus monodon*, as part of the host defense mechanism, against *Vibrio harveyi* infection (Soonthornchai et al., 2010). Our data also indicated that fourteen mucin genes are induced in the WSSV-infected intestine organ of *M. japonicus*, suggesting that these mucins may be involved in antiviral responses.

Peritrophin was first identified in the peritrophic membrane of insect, which was thought to play important roles in facilitating digestion and preventing microorganism invasion (Lehane, 1997; Tellam et al., 1999; Hegedus et al., 2009). It has been shown recently that peritrophin-like gene also exists in crustaceans. Two peritrophin-like proteins have protection roles around eggs after fertilization in *Penaeus semisulcatus* (Khayat et al., 2001). A peritrophin-like gene from fleshy shrimp (*Fenneropenaeus chinensis*) could bind chitin and Gram-negative bacteria (Du et al., 2006). Another ovarian peritrophin from *Fenneropenaeus merguiensis* was shown to have antimicrobial activity (Loongyai et al., 2007). Moreover, a new shrimp peritrophin-like gene from *Exopalaemon carinicauda* was demonstrated to be involved in WSSV infection (Wang et al., 2013). In this study, three peritorphin-like genes from the *M. japonicus* intestine tissue were found to be up-

Table 4
Up-regulated DEGs associated with immune responses during WSSV infection.

Gene id.	Accession no.	Gene description	Species	Fold changes*
mucin				
CL227.Contig4_All	gi|762091145|	mucin-2-like isoform X1	*Crassostrea gigas*	10.34318572
Unigene20320_All	gi|795498118|	mucin-19-like	*Cercocebus atys*	10.28193003
Unigene19170_All	gi|795498118|	mucin-19-like	*Cercocebus atys*	9.413627929
CL1035.Contig2_All	gi|684412208|	mucin-5B-like	*Opisthorchis viverrini*	8.13442632
Unigene16743_All	gi|731251885|	mucin-2-like	*Fukomys damarensis*	7.714245518
CL3093.Contig2_All	gi|795498118|	mucin-19-like	*Cercocebus atys*	7.139551352
CL2012.Contig1_All	gi|900916353|	mucin-2	*Drosophila simulans*	2.411195433
CL2850.Contig2_All	gi|56283929|	mucin-2	*Drosophila melanogaster*	2.26388081
CL1258.Contig1_All	gi|805779225|	mucin-17-like	*Megachile rotundata*	2.091651459
Unigene6342_All	gi|944345637|	mucin-2	*Alligator sinensis*	1.944069972
CL1258.Contig3_All	gi|805779225|	mucin-17-like	*Megachile rotundata*	1.827881562
CL4068.Contig1_All	gi|950963036|	mucin-1	*Alligator mississippiensis*	1.7093491
Unigene19467_All	gi|688616184|	mucin-2-like	*Danio rerio*	1.346450414
CL2073.Contig1_All	gi|525003284|	mucin-3A-like	*Ficedula albicollis*	1.291199137
peritrophin				
CL998.Contig3_All	gi|149689492|	cortical rod-like protein	*Macrobrachium rosenbergii*	2.628284303
Unigene11308_All	gi|57157484|	cortical rod protein	*Marsupenaeus japonicus*	2.515838198
Unigene11310_All	gi|57157486|	cortical rod protein-2	*Marsupenaeus japonicus*	2.463968017
cytochrome c oxidase				
Unigene20638_All	gi|671184726|	cytochrome c oxidase subunit I	*Sus scrofa*	7.451211112
Unigene1757_All	gi|700894663|	mitochondrial cytochrome c oxidase subunit VIc	*Litopenaeus vannamei*	1.670322076
CL1764.Contig2_All	gi|926635335|	cytochrome c oxidase assembly factor 5-like	*Limulus polyphemus*	1.505222151
Unigene12726_All	gi|478258154|	cytochrome c oxidase subunit 8	*Dendroctonus ponderosae*	1.03687088
chitinase				
CL227.Contig2_All	gi|270297196|	chitinase	*Tribolium castaneum*	7.584962501
CL745.Contig2_All	gi|926627062|	acidic mammalian chitinase-like	*Limulus polyphemus*	7.17990909
CL227.Contig1_All	gi|780699813|	chitinase	*Wasmannia auropunctata*	6.844095469
exportin				
CL527.Contig1_All	gi|936683959|	exportin-1 isoform X2	*Trichogramma pretiosum*	6.357552005
CL1712.Contig3_All	gi|939661979|	exportin-7 isoform X2	*Microplitis demolitor*	1.067114196
ALF				
Unigene16422_All	gi|988045884|	Anti-lipopolysaccharide factor	*Marsupenaeus japonicus*	2.158958989
Unigene7059_All	gi|988045882|	Anti-lipopolysaccharide factor	*Marsupenaeus japonicus*	1.959107569
MIF				
Unigene14734_All	gi|480813569|	macrophage migration inhibitory factor	*Litopenaeus vannamei*	1.006719598
caspase				
CL2600.Contig1_All	gi|304569876|	caspase	*Eriocheir sinensis*	1.210035215
Unigene11800_All	gi|89272782|	caspase	*Xenopus tropicalis*	3.707359132
syndecan				
CL823.Contig3_All	gi|557233992|	syndecan 3	*Eimeria brunetti*	3.36923381
CL900.Contig1_All	gi|807119195|	syndecan 2	*Litopenaeus vannamei*	1.412383046
VEGF				
CL992.Contig1_All	gi|926625265|	vascular endothelial growth factor A-like	*Limulus polyphemus*	6.189824559
Unigene11742_All	NA	VEGF dmain	NA	2.396695863
TPS				
Unigene4177_All	gi|189031345|	trehalose-6-phosphate synthase	*Fenneropenaeus chinensis*	1.467986379
Unigene15767_All	gi|189031345|	trehalose-6-phosphate synthase	*Fenneropenaeus chinensis*	1.154262601
C-type lectin				
Unigene19494_All	gi|76781670|	C-type lectin 1	*Fenneropenaeus chinensis*	9.025139562
CL2474.Contig2_All	gi|387165444|	C-type lectin 2	*Marsupenaeus japonicus*	7.276124405
Rho GTPase				
CL1605.Contig4_All	gi|936703116|	Rho GTPase-activating protein 20	*Trichogramma pretiosum*	7.483815777
CL4779.Contig2_All	gi|312083445|	Rho GTPase-activating protein gacF-like	*Loa loa*	2.462069891
fibrinogen				
CL2097.Contig1_All	gi|936626702|	fibrinogen-related protein isoform 1	*Litopenaeus vannamei*	7.426264755
SAM and SH				
CL2097.Contig1_All	gi|815803049|	SAM and SH3 domain-containing protein 1-like	*Linepithema humile*	5.95419631
VASP				
CL3772.Contig2_All	gi|556963374|	vasodilator-stimulated phosphoprotein isoform X3	*Latimeria chalumnae*	2.102810806

* Fold changes is log2 ratio in gene expression.

regulated in WSSV infection group. All these results suggested that the peritrophins may play a role in immune defense.

Cytochrome c oxidase is a mitochondrial apoptogenic factor, which is also involved in pathogenic infection. For instance, dopamine-induced programmed cell death is associated with cytochrome c oxidase release and caspase 3 activation (Pirger et al., 2009). In addition, the expression of cytochrome c oxidase was also induced after WSSV infection in red claw crayfish (*Cherax quadricarinatus*) (Liu et al., 2011) and Pacific white shrimp (*Litopenaeus vannamei*) (Hu et al., 2016). The present transcriptome data reveal that at least four cytochrome c oxidases are responded to WSSV infection in the intestine organ of *M. japonicus*, suggesting their potential immune characteristics.

In crustaceans, chitin is the major components of shell, which can not only provide mechanical rigidity to extracellular structure, but also form a physical barrier against invading microorganisms (Mali et al., 2004). Chitinase is a kind of glycosyl hydrolases that can randomly hydrolyze the β-1,4-glycosidic bonds of chitin and then produce N-acetylchitooli-gosaccharides. Previous studies have demonstrated that chitinase plays an important role in defense against pathogens. In *Crassostrea gigas*, chitinase is involved in early embryonic development

and immune response (Badariotti et al., 2007). And the expression levels of chitinases were up-regulated in *Penaeus japonicus* and *Exopalaemon carinicauda* against *Vibrio anguillarum* or WSSV challenge (Pan et al., 2005; Duan et al., 2014). Our transcriptome data also indicate that several chitinases are up-regulated under WSSV infection in the intestine organ of *M. japonicus*. The results suggested that chitinases may participate in the immune defenses to pathogen infection.

Anti-lipopolysaccharide factor (ALF) is a cationic antimicrobial peptide, which can bind and neutralize lipopolysaccharide and plays key roles in innate immunity (Aketagawa et al., 1986). ALF was first identified from *Limulus polyphemus* (Muta et al., 1987). Structurally, ALFs have a LPS-binding domain and a disulphide loop formed by two conserved cysteine residues, which are considered to be the key functional domain for antibacterial activity (Aketagawa et al., 1986). Some recombinant ALFs and synthetic LPS-binding domain exhibited different antimicrobial activities (Liu et al., 2006; Tharntada et al., 2009; Liu et al., 2012; Yang et al., 2016; Lin et al., 2016). Not only that, ALFs also performed antiviral activities. For instance, recombinant ALF proteins from *Penaeus monodon* and *Cherax quadricarinatus* exerted anti-WSSV activity (Suraprasit et al., 2014; Lin et al., 2016). We also found that expression levels of two *ALFs* from *M. japonicus* were up-regulated by WSSV. All of these data suggest that ALFs play important roles in immune defence against microbial infection.

As a multifunctional transmembrane protein, syndecan is considered to function as a cell surface receptor involved in cell adhesion, migration, cytoskeleton organization and differentiation (Carey, 1997; Rapraeger, 2001). It can bind a wide variety of extracellular molecules to regulate the biological activity of the organisms. Some pathogenic bacteria can utilize syndecan to bind to the cell surface (Kim et al., 2004). During an inflammatory response, the expression level of the syndecan can be enhanced (Zhang et al., 1999). Syndecan was also reported to interact with WSSV in the Pacific white shrimp *Litopenaeus vannamei* (Yang et al., 2015). After silencing of a syndecan with siRNA, the WSSV copy numbers and mortality of shrimp after WSSV infection were both significantly decreased. Moreover, the transcription level of the syndecan was apparently up-regulated after WSSV challenge (Yang et al., 2015). This result is similar to our transcriptional data (Table 4). These data provide useful information for understanding the immune mechanism of the syndecan involved in WSSV infection.

Rho GTPase was first identified in yeast, which is an important component of the endomembrane system (Salminen and Novick, 1987). Usually, Rho GTPase has two conformations: one is GDP-binding inactive conformation, another is GTP-binding active conformation (Ohbayashi and Fukuda, 2012). Moreover, two conformations can be shuttled. In the active conformation, Rho GTPase can interact with various proteins and regulate membrane trafficking (Segev, 2001). Previous studies have indicated that Rho GTPases play important roles in crustacean innate immunity. For instance, expression level of the *PjRab* gene was up-regulated after WSSV infection in *Penaeus japonicus* (Wu and Zhang, 2007). By interacting with β-actin and tropomyosin, Rho GTPase can regulate shrimp hemocytic phagocytosis of WSSV (Wu et al., 2007). In *Penaeus monodon*, Rho GTPase can directly interact with VP28 in systemic infection of WSSV (Sritunyalucksana et al., 2006). In addition, after challenged with WSSV and *Vibrio parahaemolyticus*, the expression levels of all 11 *MrRabs* were up-regulated, indicating that they were involved in prawns antibacterial immunity (Huang and Ren, 2015). The current study also indicated that two Rho GTPases *were up-regulated after the* intestine organ infecting with WSSV, suggesting their potential immunity. In addition to the above genes, we also observed the activation of *exportin*, *macrophage migration inhibitory factor*, *caspase*, *vascular endothelial growth factor*, *trehalose-6-phosphate synthase*, *C-type lectin*, *fibrinogen*, *SAM* and *SH3 domain-containing protein*, and *vasodilator-stimulated phosphoprotein* in the intestine organ of *M. japonicus* after the WSSV challenge (Table 4).

4. Conclusions

In this study, we performed *de novo* transcriptome sequencing of the intestine organ in *M. japonicus*. And a total of 63,458 and 44,350 unigenes were obtained in the mock and WSSV-infected samples, respectively. Among 12,920 identified DEGs, 675 genes were up-regulated when comparing the infection samples with the control. Comparative transcriptome analysis of these samples indicated that multiple genes were involved in WSSV tolerance. This study will provide useful information for crustacean intestine immune.

Acknowledgements

The current study was supported by the National Natural Science Foundation of China (Grant Nos. 31702370, 31572647), the Natural Science Foundation of Jiangsu Province (BK20171474), Natural Science Fund of Colleges and universities in Jiangsu Province (16KJD240001, 14KJA240002), and the Project Funded by the Priority Academic Program Development of Jiangsu Higher Education Institutions (PAPD).

Appendix A. Supplementary data

Supplementary material related to this article can be found, in the online version, at doi:https://doi.org/10.1016/j.vetimm.2018.12.001.

References

Aketagawa, J., Miyata, T., Ohtsubo, S., Nakamura, T., Morita, T., et al., 1986. Primary structure of limulus anticoagulant anti-lipopolysaccharide factor. J. Biol. Chem. 261, 7357–7365.

Badariotti, F., Thuau, R., Lelong, C., Dubos, M.P., Favrel, P., 2007. Characterization of an atypical family 18 chitinase from the oyster *Crassostrea gigas*: evidence for a role in early development and immunity. Dev. Comp. Immunol. 31 (6), 559–570.

Cao, J., Wu, L., Jin, M., Li, T., Hui, K., Ren, Q., 2017. Transcriptome profiling of the *Macrobrachium rosenbergii* lymphoid organ under the white spot syndrome virus challenge. Fish Shellfish Immunol. 67, 27–39.

Carey, D., 1997. Syndecans: multifunctional cell-surface co-receptors. Biochem. J. 327, 1–16.

Chen, Y.H., Yuan, F.H., Bi, H.T., Zhang, Z.Z., Yue, H.T., et al., 2016. Transcriptome analysis of the unfolded protein response in hemocytes of Litopenaeus vannamei. Fish Shellfish Immunol. 54, 153–163.

Conesa, A., Götz, S., García-Gómez, J.M., Terol, J., Talón, M., Robles, M., 2005. Blast2GO: a universal tool for annotation, visualization and analysis in functional genomics research. Bioinformatics 21 (18), 3674–3676.

Du, X.J., Wang, J.X., Liu, N., Zhao, X.F., Li, F.H., Xiang, J.H., 2006. Identification and molecular characterization of a peritrophin-like protein from fleshy prawn (*Fenneropenaeus chinensis*). Mol. Immunol. 43 (10), 1633–1644.

Duan, Y., Liu, P., Li, J., Li, J., Wang, Y., Chen, P., 2014. The responsive expression of a chitinase gene in the ridgetail white prawn *Exopalaemon carinicauda* against *Vibrio anguillarum* and WSSV challenge. Cell Stress Chaperones 19 (4), 549–558.

Faderl, M., Noti, M., Corazza, N., Mueller, C., 2015. Keeping bugs in check: the mucus layer as a critical component in maintaining intestinal homeostasis. IUBMB Life 67 (4), 275–285.

Gill, N., Wlodarska, M., Finlay, B.B., 2010. The future of mucosal immunology: studying an integrated system-wide organ. Nat. Immunol. 11 (7), 558–560.

Grabherr, M.G., Haas, B.J., Yassour, M., Levin, J.Z., Thompson, D.A., et al., 2011. Full-length transcriptome assembly from RNA-Seq data without a reference genome. Nat. Biotechnol. 29 (7), 644–652.

Hartmann, P., Chen, P., Wang, H.J., Wang, L., McCole, D.F., et al., 2013. Deficiency of intestinal mucin-2 ameliorates experimental alcoholic liver disease in mice. Hepatology 58 (1), 108–119.

Hasnain, S.Z., Gallagher, A.L., Grencis, R.K., Thornton, D.J., 2013. A new role for mucins in immunity: insights from gastrointestinal nematode infection. Int. J. Biochem. Cell Biol. 45 (2), 364–374.

Hegedus, D., Erlandson, M., Gillott, C., Toprak, U., 2009. New insights into peritrophic matrix synthesis, architecture, and function. Annu. Rev. Entomol. 54, 285–302.

Hu, W.Y., Yao, C.L., 2016. Molecular and immune response characterizations of a novel AIF and cytochrome c in *Litopenaeus vannamei* defending against WSSV infection. Fish Shellfish Immunol. 56, 84–95.

Huang, Y., Ren, Q., 2015. Identification and function of 11 Rab GTPases in giant freshwater prawn Macrobrachium rosenbergii. Fish Shellfish Immunol. 43 (1), 120–130.

Johansson, M.E., Hansson, G.C., 2016. Immunological aspects of intestinal mucus and mucins. Nat. Rev. Immunol. 16 (10), 639–649.

Khayat, M., Babin, P.J., Funkenstein, B., Sammar, M., Nagasawa, H., et al., 2001. Molecular characterization and high expression during oocyte development of a shrimp ovarian cortical rod protein homologous to insect intestinal peritrophins. Biol.

Reprod. 64 (4), 1090–1099.
Kim, H.R., Choi, M.S., Kim, I.S., 2004. Role of Syndecan-4 in the cellular invasion of Orientia tsutsugamushi. Microb. Pathog. 36, 219–225.
Koiwai, K., Kondo, H., Hirono, I., 2018a. RNA-seq identifies integrin alpha of kuruma shrimp *Marsupenaeus japonicus* as a candidate molecular marker for phagocytic hemocytes. Dev. Comp. Immunol. 81, 271–278.
Koiwai, K., Kondo, H., Hirono, I., 2018b. The immune functions of sessile hemocytes in three organs of kuruma shrimp *Marsupenaeus japonicus* differ from those of circulating hemocytes. Fish Shellfish Immunol. 78, 109–113.
Lang, T., Hansson, G.C., Samuelsson, T., 2007. Gel-forming mucins appeared early in metazoan evolution. Proc. Natl. Acad. Sci. U. S. A. 104 (41), 16209–16214.
Lehane, M.J., 1997. Peritrophic matrix structure and function. Annu. Rev. Entomol. 42, 525–550.
Lin, F.Y., Gao, Y., Wang, H., Zhang, Q.X., Zeng, C.L., Liu, H.P., 2016. Identification of an anti-lipopolysacchride factor possessing both antiviral and antibacterial activity from the red claw crayfish Cherax quadricarinatus. Fish Shellfish Immunol. 57, 213–221.
Liu, H., Jiravanichpaisal, P., Söderhäll, I., Cerenius, L., Söderhäll, K., 2006. Antilipopolysaccharide factor interferes with white spot syndrome virus replication in vitro and in vivo in the crayfish Pacifastacus leniusculus. J. Virol. 80 (21), 10365–10371.
Liu, H.P., Chen, R.Y., Zhang, Q.X., Peng, H., Wang, K.J., 2011. Differential gene expression profile from haematopoietic tissue stem cells of red claw crayfish, *Cherax quadricarinatus*, in response to WSSV infection. Dev. Comp. Immunol. 35 (7), 716–724.
Liu, H.P., Chen, R.Y., Zhang, Q.X., Wang, Q.Y., Li, C.R., et al., 2012. Characterization of two isoforms of antiliopolysacchride factors (Sp-ALFs) from the mud crab Scylla paramamosain. Fish Shellfish Immunol. 33, 1–10.
Livak, K.J., Schmittgen, T.D., 2001. Analysis of relative gene expression data using real-time quantitative PCR and the 2(T)(-Delta Delta C) method. Methods 25, 402–408.
Lo, C.F., Ho, C.H., Peng, S.E., Chen, C.H., Hsu, H.C., et al., 1996. White spot syndrome baculovirus (WSBV) detected in cultured and captured shrimp, crabs and other arthropods. Dis. Aquat. Org. 27, 215–225.
Loongyai, W., Avarre, J.C., Cerutti, M., Lubzens, E., Chotigeat, W., 2007. Isolation and functional characterization of a new shrimp ovarian peritrophin with antimicrobial activity from Fenneropenaeus merguiensis. Mar. Biotechnol. (NY) 9 (5), 624–637.
Mali, B., Möhrlen, F., Frohme, M., Frank, U., 2004. A putative double role of a chitinase in a cnidarian: pattern formation and immunity. Dev. Comp. Immunol. 28 (10), 973–981.
McAuley, J.L., Linden, S.K., Png, C.W., King, R.M., Pennington, H.L., et al., 2007. MUC1 cell surface mucin is a critical element of the mucosal barrier to infection. J. Clin. Invest. 117 (8), 2313–2324.
McGuckin, M.A., Every, A.L., Skene, C.D., Linden, S.K., Chionh, Y.T., 2007. Muc1 mucin limits both *Helicobacter pylori* colonization of the murine gastric mucosa and associated gastritis. Gastroenterology 133 (4), 1210–1218.
McGuckin, M.A., Lindén, S.K., Sutton, P., Florin, T.H., 2011. Mucin dynamics and enteric pathogens. Nat. Rev. Microbiol. 9 (4), 265–278.
Ménard, S., Cerf-Bensussan, N., Heyman, M., 2010. Multiple facets of intestinal permeability and epithelial handling of dietary antigens. Mucosal Immunol. 3 (3), 247–259.
Mortazavi, A., Williams, B.A., McCue, K., Schaeffer, L., Wold, B., 2008. Mapping and quantifying mammalian transcriptomes by RNA-Seq. Nat. Methods 5 (7), 621–628.
Muta, T., Miyata, T., Tokunaga, F., Nakamura, T., Iwanaga, S., 1987. Primary structure of anti-lipopolysaccharide factor from American horseshoe crab, Limulus polyphemus. J. Biochem. 101, 1321–1330.
Mutz, K.O., Heilkenbrinker, A., Lönne, M., Walter, J.G., Stahl, F., 2013. Transcriptome analysis using next-generation sequencing. Curr. Opin. Biotechnol. 24 (1), 22–30.
Ohbayashi, N., Fukuda, M., 2012. Role of Rab family GTPases and their effectors in melanosomal logistics. J. Biol. Chem. 151, 343–351.
Pan, D., He, N., Yang, Z., Liu, H., Xu, X., 2005. Differential gene expression profile in hepatopancreas of WSSV-resistant shrimp (*Penaeus japonicus*) by suppression subtractive hybridization. Dev. Comp. Immunol. 29 (2), 103–112.
Pirger, Z., Rácz, B., Kiss, T., 2009. Dopamine-induced programmed cell death is associated with cytochrome c release and caspase-3 activation in snail salivary gland cells. Biol. Cell 101 (2), 105–116.
Rao, R., Bing, Zhu.Y., Alinejad, T., Tiruvayipati, S., Lin, Thong.K., Wang, J., Bhassu, S., 2015. RNA-seq analysis of *Macrobrachium rosenbergii* hepatopancreas in response to Vibrio parahaemolyticus infection. Gut Pathog. 7, 6.
Rapraeger, A.C., 2001. Molecular interactions of syndecans during development. Semin. Cell Dev. Biol. 12, 107–116.
Salminen, A., Novick, P.J., 1987. Aras-like protein is required for a post-Golgi event in yeast secretion. Cell 49, 527–538.
Schlicker, A., Domingues, F.S., Rahnenfuhrer, J., Lengauer, T., 2006. A new measure for functional similarity of gene products based on Gene Ontology. BMC Bioinf. 7 (1), 302.
Segev, N., 2001. Ypt and Rab GTPases: insight into functions through novel interactions. Curr. Opin. Cell Biol. 13 (4), 500–511.
Seibert, C.H., Pinto, A.R., 2012. Challenges in shrimp aquaculture due to viral diseases: distribution and biology of the five major penaeid viruses and interventions to avoid viral incidence and dispersion. Braz. J. Microbiol. 43 (3), 857–864.
Soonthornchai, W., Rungrassamee, W., Karoonuthaisiri, N., Jarayabhand, P., Klinbunga, S., et al., 2010. Expression of immune-related genes in the digestive organ of shrimp, *Penaeus monodon*, after an oral infection by *Vibrio harveyi*. Dev. Comp. Immunol. 34 (1), 19–28.
Sritunyalucksana, K., Wannapapho, W., Lo, C.F., Flegel, T.W., 2006. PmRab7 is a VP28-binding protein involved in white spot syndrome virus infection in shrimp. J. Virol. 80, 10734–10742.
Suraprasit, S., Methatham, T., Jaree, P., Phiwsaiya, K., Senapin, S., et al., 2014. Anti-lipopolysaccharide factor isoform 3 from *Penaeus monodon* (ALFPm3) exhibits antiviral activity by interacting with WSSV structural proteins. Antiviral Res. 110, 142–150.
Tellam, R.L., Wijffels, G., Willadsen, P., 1999. Peritrophic matrix proteins. Insect Biochem. Mol. Biol. 29 (2), 87–101.
Tharntada, S., Ponprateep, S., Somboonwiwat, K., Liu, H., Söderhäll, I., Söderhäll, K., Tassanakajon, A., 2009. Role of anti-lipopolysaccharide factor from the black tiger shrimp, *Penaeus monodon*, in protection from white spot syndrome virus infection. J. Gen. Virol. 90 (Pt 6), 1491–1498.
Velcich, A., Yang, W., Heyer, J., Fragale, A., Nicholas, C., 2002. Colorectal cancer in mice genetically deficient in the mucin Muc2. Science 295 (5560), 1726–1729.
Wang, Y.C., Lo, C.F., Chang, P.S., Kou, G.H., 1998. Experimental infection of white spot baculovirus in some cultured and wild decapods in Taiwan. Aquaculture 164, 221–231.
Wang, L., Li, F., Wang, B., Xiang, J., 2013. A new shrimp peritrophin-like gene from *Exopalaemon carinicauda* involved in white spot syndrome virus (WSSV) infection. Fish Shellfish Immunol. 35 (3), 840–846.
Wittig, B.M., Zeitz, M., 2003. The gut as an organ of immunology. Int. J. Colorectal Dis. 18 (3), 181–187.
Wu, W., Zong, R., Xu, J., Zhang, X., 2007. Antiviral phagocytosis is regulated by a novel Rab-dependent complex in shrimp Penaeus japonicus. J. Proteome Res. 7, 424–431.
Wu, W.L., Zhang, X.B., 2007. Characterization of a Rab GTPase up-regulated in the shrimp *Peneaus japonicus* by virus infection. Fish Shellfish Immunol. 23, 438–445.
Yan, L., Yang, C., Tang, J., 2013. Disruption of the intestinal mucosal barrier in *Candida albicans* infections. Microbiol. Res. 168 (7), 389–395.
Yang, H., Li, S., Li, F., Wen, R., Xiang, J., 2015. Analysis on the expression and function of syndecan in the Pacific white shrimp Litopenaeus vannamei. Dev. Comp. Immunol. 51 (2), 278–286.
Yang, H., Li, S., Li, F., Xiang, J., 2016. Structure and bioactivity of a modified peptide derived from the LPS-binding domain of an anti-lipopolysaccharide factor (ALF) of shrimp. Mar. Drugs 14, 96.
Ye, T., Tang, W., Zhang, X., 2012. Involvement of Rab6 in the regulation of phagocytosis against virus infection in invertebrates. J. Proteome Res. 11, 4834–4846.
Zhang, Y., Pasparakis, M., Kollias, G., Simons, M., 1999. Myocyte-dependent regulation of endothelial cell syndecan-4 expression ROLE OF TNF-α. J. Biol. Chem. 274, 14786–14790.
Zhong, S., Mao, Y., Wang, J., Liu, M., Zhang, M., Su, Y., 2017. Transcriptome analysis of Kuruma shrimp (*Marsupenaeus japonicus*) hepatopancreas in response to white spot syndrome virus (WSSV) under experimental infection. Fish Shellfish Immunol. 70, 710–719.